C-Glycosyl Bond Conformation in Oxazofurin: Crystallographic and Computational Studies of the Oxazole Analogue of Tiazofurin

Barry M. Goldstein,*,† Hong Li,† Wendy H. Hallows,†,⊥ David A. Langs,‡ Palmarisa Franchetti,§ Loredana Cappellacci,§ and Mario Grifantini§

Department of Biophysics, University of Rochester Medical Center, Rochester, New York 14642, Medical Foundation of Buffalo, 73 High Street, Buffalo, New York 14203, and Dipartimento di Scienze Chimiche, Università di Camerino, 62032 Camerino, Italy

Received October 15, 1993®

Oxazofurin is the inactive oxazole analogue of the C-glycosyl thiazole antitumor agent tiazofurin. Replacement of the thiazole sulfur in tiazofurin with the oxazole oxygen in oxazofurin produces conformational effects that are examined using crystallographic and computational methods. The crystal structure of oxazofurin contains six molecules in the asymmetric unit and has been refined to a standard R value of 6.8% for all data. The six oxazofurin conformers show an average C-glycosidic torsion angle of 70(9)°. This value is significantly higher than the average absolute C-glycosidic torsion angle of 24(10)° obtained from previous thiazole nucleoside structures. Previous studies suggest that, in tiazofurin, an electrostatic interaction between a positively charged thiazole sulfur and negatively charged furanose oxygen constrains the C-glycosidic torsion angle to a relatively small value. *Ab initio* molecular orbital studies presented here suggest that the higher C-glycosidic angles observed in the oxazofurin structures result from a repulsive interaction between negatively charged oxazole and furanose oxygens. Thus, it is likely that differences in activity between oxazo- and tiazofurin are either (1) due directly to differences in electronic properties between the thiazole and oxazole rings or (2) due to the variation in C-glycosidic bond conformation resulting from the alteration in the charge distribution of the heterocycle.

Introduction

Tiazofurin (NSC 286193) is a thiazole-containing C-nucleoside which has demonstrated clinical efficacy in the treatment of human leukemias.[1-3] The antitumor activity of tiazofurin results from a combination of cytotoxic and maturation-inducing activities.[2-4] Both effects result from inhibition of the target enzyme inosine monophosphate dehydrogenase (IMPd)[2-4] by the tiazofurin anabolite thiazole-4-carboxamide adenine dinucleotide (TAD).[5,6]

Close contacts between the thiazole sulfur and furanose oxygen are observed in crystal structures of free tiazofurin[7] and enzyme-bound TAD analogues,[8] suggesting that a nonbonded S···O interaction may be one requirement for activity in the thiazole nucleosides. Constraints imposed by this interaction on rotation about the C-glycosyl bond may enhance binding of tiazofurin or an intermediate to anabolic enzymes or enhance binding of TAD to the target IMPd. Oxazofurin (1), the inactive oxazole analogue of tiazofurin,[9] thus provides an ideal control for examining the significance of the S···O interaction.

Computational[10] and data base[11] studies suggest that the close S–O contact observed in tiazofurin results from an electrostatic interaction between a positively charged sulfur and negatively charged oxygen. In oxazofurin, replacement of the divalent thiazole sulfur by the more electronegative oxygen may be expected to compromise this interaction and thus alter the conformation about the C-glycosidic bond. In order to test this hypothesis, the crystal structure of oxazofurin has been determined. This novel structure yields six crystallographically independent molecules in the asymmetric unit, hence six independent determinations of the C-glycosidic torsion angle. *Ab inito* molecular orbital studies also examine the electronic structure of the oxazole ring and its influence on C-glycosyl bond conformation. Comparison of results from oxazofurin with those from the thiazole nucleosides supports the contention that C-glycosyl bond conformation may be an important determinant of activity in the substituted C-nucleosides.

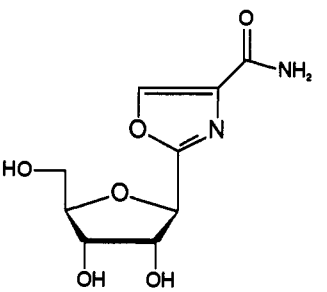

(1)

Results and Discussion

1. Crystallographic Studies. The crystal structure of oxazofurin is shown in Figure 1. Crystal and refinement data are summarized in Table 1. This structure contains six molecules in the asymmetric unit. Thus, the crystal structure provides six crystallographically independent determinations of the molecular conformation of oxazofurin. This finding is particularly valuable in that constrained regions of the molecule can be more easily identified. Each conformer is subjected to different intermolecular packing interactions. Thus, structural features which are conserved among the six conformers are more likely to result from intramolecular interactions and are more likely to be conserved in solution.[12]

* Author to whom correspondence should be addressed.
† University of Rochester Medical Center.
‡ Medical Foundation of Buffalo.
§ Università di Camerino.
⊥ Current address: Department of Chemistry, Rochester Institute of Technology, 1 Lomb Memorial Drive, Rochester, NY 14623.
® Abstract published in *Advance ACS Abstracts*, April 15, 1994.

0022-2623/94/1837-1684$04.50/0

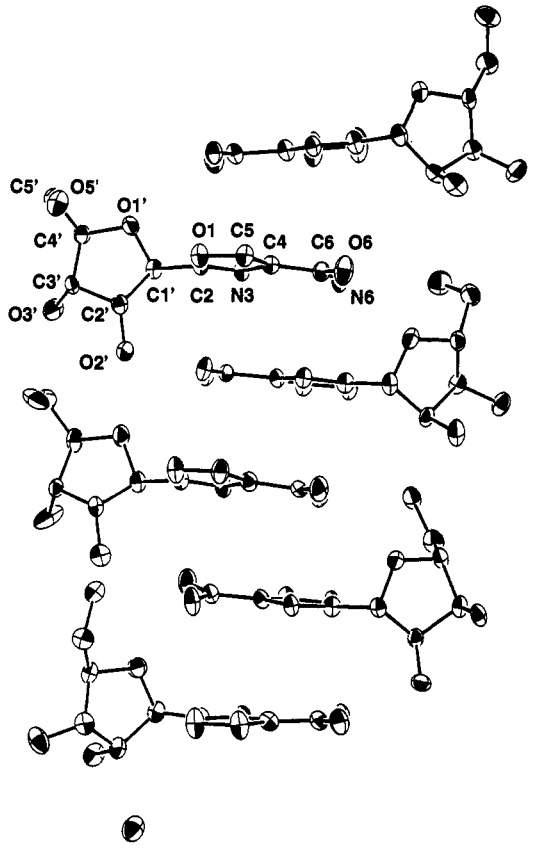

Figure 1. Asymmetric unit of the oxazofurin crystal structure showing the six molecular conformers. Conformers are numbered sequentially from the top of the figure for comparison with Table 2. Atom labels are shown for conformer 2. Hydrogen atoms are omitted for clarity. Non-hydrogen atoms are represented by thermal ellipsoids at the 50% probability level. The unattached atom at bottom is the oxygen of the water of hydration.

Table 1. Crystal Data and Data Collection and Refinement Variables for Oxazofurin

formula	$C_9H_{12}N_2O_6 \cdot {}^1/_6H_2O$
M_r	247.2
space group	monoclinic, $P2_1$
a (Å)	5.482(1)
b (Å)	29.423(4)
c (Å)	19.546(2)
β (°)	91.04(1)
Z	12
crystal size (mm)	0.07 × 0.07 × 0.62
diffractometer	Enraf-Nonius CAD4
scan type	ω–2θ
radiation	CuKα (λ = 1.5418 Å)
lattice parameter refinement	25 rflns ($23.8 < 2\theta < 61.4°$)
transmission factor (on I)	0.867–1.000
data collection range: θ	$3° < 2\theta < 156°$
data collection range: h,k,l	$0 \le h \le 6$; $0 \le k \le 37$; $-24 \le l \le 24$
total reflections	7493
unique reflections	6774 ($5307 > 3\sigma(F_o)$)
$R_{merge}(I)$	0.035
$R_{merge}(F)$	0.028
$R(F)$ (all data)	0.068
$R_w(F)$ (all data)	0.067
no. variables	1186
S	1.026
$(\Delta/\sigma)_{max}$	0.53
extinction parameter G ($\times 10^{-4}$)	0.41

The number of independent molecules seen in this crystal structure is unusual. A search of the Cambridge structural database (version 4.5)[12] yields only 39 structures which contain six or more molecules in the asymmetric unit from a total of ~100 000 entries. Of these, none are nucleosides. In fact, this is the first furanose-containing crystal structure to demonstrate more than four molecules in the asymmetric unit.

Atomic coordinates and individual bond lengths and angles for the six oxazofurin conformers are deposited. Sugar puckers[13] and selected torsion angles for each conformer are listed in Table 2. These values provide general structural features of each molecule.

The oxazole ring in each conformer is planar within experimental error. Average bond lengths and angles in the oxazofurin oxazole rings are comparable to those obtained from a Cambridge structural database search of 26 previously determined oxazole structures (deposited). Values of the carboxamide torsion angle κ (Table 2) indicate that the carboxamide amino group in each structure is approximately *cis*-planar to the oxazole nitrogen. This is the same conformation seen in all thiazole nucleoside structures.[14] The oxazole carboxamide group is likely constrained in an approximate *cis*-planar conformation by intramolecular N6–H···N3 and O6···H interactions similar to those identified in the thiazole-4-carboxamide moiety.[14]

The conformational feature of greatest interest is the C-glycosidic torsion angle χ_o, defined by the atoms O1–C2–C1′–O1′. Values of χ_o for the six conformers range between 58° and 83° (Table 2). Thus, the same general *anti* conformation is seen in all six independent molecules, despite variations in sugar pucker and 5′-hydroxyl orientation (Table 2). This finding suggests that the C-glycosidic torsion angle in oxazofurin is at least partially constrained within an ~25° range.

Values of χ_o may be compared with those of the analogous C-glycosidic torsion angle χ_s observed in the thiazole nucleosides, defined by atoms S1–C2–C1′–O1′. Absolute values of χ_s for 11 independent thiazole nucleoside structures[7,10,15] range between 5.2° and 40.8°, with one outlier at 55.2° (ara-tiazofurin, below).[16] Values of χ_o and χ_s are compared graphically in the polar plot shown in Figure 2. Each point represents the conformation of one oxazole or thiazole nucleoside. The radial distance of each point from the origin represents the distance between the furanose oxygen O1′ and the oxazole or thiazole heteroatom (O1 or S1). The angle between this radius and the horizontal axis gives the absolute value of χ_o or χ_s. The mean value of χ_o is 70(9)° vs a mean of 24(10)° for χ_s in the thiazole nucleosides (omitting the ara-tiazofurin structure). It is apparent from Figure 2 that the oxazole ring in oxazofurin adopts significantly higher C-glycosidic torsion angles than does the thiazole moiety in tiazofurin and its analogues.

Crystallographic and computational studies suggest that the C-glycosidic bond in tiazofurin is constrained such that the thiazole sulfur is generally *syn* to the furanose oxygen.[7,10,15] This constraint results from the combination of attractive electrostatic interactions between the positively charged sulfur and negatively charged oxygen, as well as repulsive interactions between the furanose oxygen and the negatively charged thiazole nitrogen.[10] The unusually high value of χ_s observed in ara-tiazofurin (55.2°) results from competing S···O1′ and S···O2′ interactions.[16]

Crystallographic results suggest that replacement of the thiazole sulfur with the oxazole oxygen removes the attractive component of the heterocycle–oxygen interaction. Apparently, repulsion between the oxazole and furanose oxygens drives the torsion angle to higher values. This hypothesis is examined next using computational studies.

Table 2. Sugar Puckers and Selected Torsion Angles (°) for the Six Oxazofurin Conformers[a]

	1	2	3	4	5	6
pucker	C3′ endo–C4′ exo	C1′ exo	C3′ endo	C1′ exo	C3′ exo	C3′ endo
ϕ (O5′–C5′–C4′–C3′)	185.6(4)	53.3(6)	59.4(7)	51.9(6)	175.7(4)	171.8(4)
κ (N3–C4–C6–N6)	0.0(8)	7.2(7)	−1.4(7)	6.7(7)	−9.0(7)	−2.8(8)
χ_o (O1–C2–C1′–O1′)	58.3(6)	62.1(5)	83.1(5)	73.5(5)	77.2(5)	68.8(6)

[a] Numbers in parentheses are standard deviations in the last significant figure.

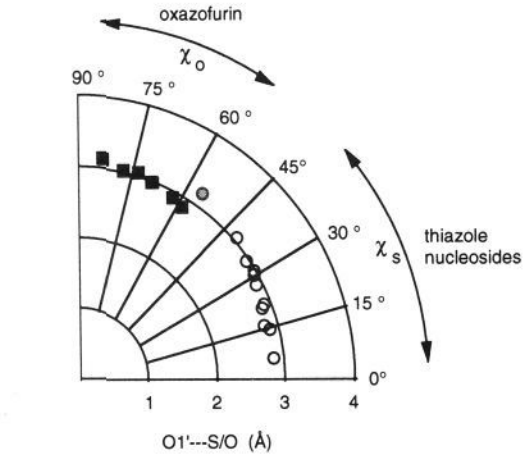

Figure 2. Polar plot comparing C-glycosidic torsion angles from the six oxazofurin conformers (χ_o) with torsion angles from the thiazole nucleosides (χ_s). Individual values of χ_o are represented by filled squares. Values of χ_s are represented by circles. The filled circle shows the outlying value of χ_s from ara-tiazofurin (see text). The radial axis gives the distance between O1′ and either S or O on the heterocycle.

2. Computational Studies. *Ab initio* quantum mechanical methods were used to identify interactions stabilizing the C-glycosidic bond conformation in oxazofurin. Electronic energy as a function of the C-glycosidic angle χ_o was determined for an oxazofurin model fragment (Figure 3). This model fragment is analogous to the thiazole nucleoside "core" fragment employed in previous computational and database studies.[10,11] The analogous oxazofurin fragment replaces the thiazole moiety with an oxazole ring. In both cases, a linkage at C2 to a methyl ester mimics the C-glycosidic bond.

Energy at a given torsion angle was obtained via full-geometry optimization at the RHF/3-21G//3-21G level.[17] Two model fragments were used. Initial optimizations were applied to a simple symmetric fragment, in which the plane of the CH3–O1′–C1′ atoms is parallel to the plane of the oxazole ring at χ_o = 0° (Figure 3). An asymmetric "ribose-like" fragment was also generated by fixing the C2–C1′–O1′–CH_3 torsion angle π at −124°, the value observed in a C3′ *endo*-puckered ribose moiety.[13] For each point on the profile, χ_o was fixed and the fragment geometry optimized (see the Experimental Section). Energy vs C-glycosidic torsion angle for each fragment is illustrated in Figure 3. A histogram of the six values of χ_o observed in the oxazofurin crystal structure is superimposed on the computational results.

General features of each curve in Figure 3 are similar. The symmetric fragment shows minima at ±60°. "Puckering" of the fragment breaks the symmetry of the curve, giving a local minimum at −60° and a global minimum at +60°. The 60° conformation is flanked by rotational barriers of ~1.5 kcal/mol at χ_o = 0° and ~2.3 kcal/mol at χ_o = 140°. This global minimum is close to the mean of the distribution of torsion angles obtained from the six oxazofurin conformations seen in the crystal structure (70(9)°).

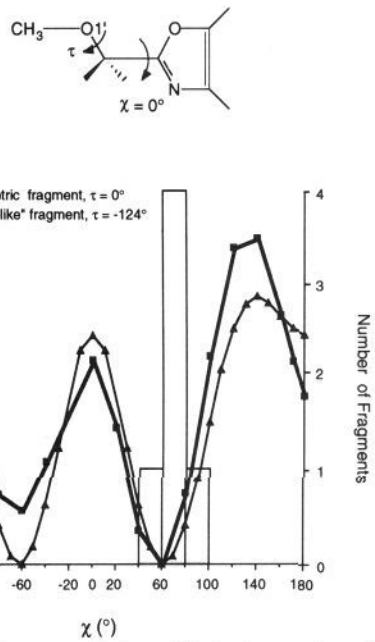

Figure 3. (left axis) Energy vs C-glycosidic torsion angle χ_o in the oxazofurin model fragment. The fragment is illustrated at top in the χ_o = 0° conformation, with τ = 0° or −124° for symmetric or ribose-like fragments respectively. Each point was obtained by fixing χ_o at the corresponding value on the horizontal axis and computing the energy for the fully optimized fragment at the RHF/3-21G//3-21G level. In each case the global minimum is normalized to 0 kcal/mol. (right axis) Histogram showing the number of conformers from the oxazofurin crystal structure with values of χ_o in the ranges indicated on the horizontal axis.

As observed in the thiazole nucleosides, the use of more complex fragments will modulate the energy curve while maintaining the basic features of the simpler models.[10] Although the location of energy minima may change as the model fragment increases in complexity, the stable conformers of oxazofurin are likely to remain at values of χ_o significantly higher than the mean of χ_s observed for the thiazole nucleosides.[10]

General features of the curves of energy vs χ_o shown in Figure 3 can be interpreted on the basis of simple electrostatic considerations. An approximate view of the electrostatic environment is obtained by examination of point charges obtained via integration and partitioning of the electron density distribution of the fragment.[17] Point charges obtained for both oxazole and thiazole fragments at the RHF/3-21G(*)//3-21G(*) level[17] are compared in Figure 4.

Charges on the thiazole fragment are comparable to those obtained previously at slightly lower levels of theory.[10] Specifically, the thiazole sulfur is positively charged and the "ribose" oxygen negatively charged. Comparison with the oxazole fragment shows that replacement of the thiazole sulfur with the oxazole oxygen introduces a large negative charge in this position on the heterocycle. Thus, the attractive electrostatic component of the S···O1′ interaction in the thiazole fragment is replaced by a repulsive O···O1′ interaction. Barriers at 0°

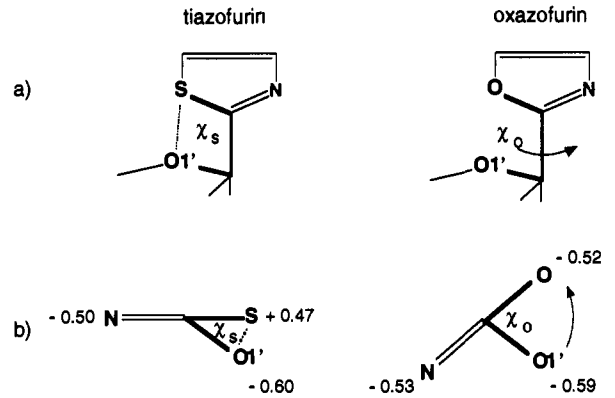

Figure 4. (a) Schematic illustration of the tiazofurin and oxazofurin model fragments. Bonds defining the C-glycosidic torsion angles χ_s and χ_o are shown in bold. (b) View down the C-glycosidic bond in both fragments with only the heteroatoms shown. Numbers next to heteroatoms are the NBO point charges computed for each fragment at the 3-21G(*)//3-21G(*) level. Electrostatic attraction between S and O1′ in tiazofurin (dotted line) produces a lower value of χ_s. Electrostatic repulsion between O and O1′ in oxazofurin increases the value of χ_o (arrow).

and ~±140° in Figure 3 reflect geometries in which the negative thiazole oxygen and nitrogen atoms are ~*cis* to the furanose oxygen. Thus, electrostatic repulsion between the furanose and oxazole oxygens produces the larger C-glycosidic angle.

Electrostatic effects are modulated by a number of less apparent charge-transfer interactions. An electrostatic model by itself would produce an energy maximum at $\chi_o = \pm 180°$, this *cis*-planar conformation yielding the closest contact between the negatively charged N3 and O1′ atoms. However, the energy profile actually shows a slight dip at $\chi_o = 180°$ in the symmetric fragment (Figure 3). Natural bond orbital analyses (not shown) indicate attractive charge-transfer interactions between bonding and antibonding orbitals centered on the C2–O and C1′–O1′ bonds. These stabilizing interactions are optimized in the 180° conformer, countering to some degree the N3···O1′ electrostatic repulsion. Similarly, a simple electrostatic model places the energy minimum at $\chi_o \sim 80°$, somewhat higher than the 60° value observed here (Figure 3). However, the 60° conformer is further stabilized by charge-transfer interactions between orbitals on the heterocycle and those on the two C1′–H bonds.

Summary and Conclusions

The crystal structure of oxazofurin is unusual, yielding six independent conformations of the molecule. These conformers have a mean C-glycosidic torsion angle of 70(9)°. This value is close to the computed global energy minimum for a "ribose-like" oxazofurin model fragment and is significantly higher than the 24(10)° mean observed for the thiazole nucleosides, omitting the ara-tiazofurin structure. A second minimum, at −60°, also differs from that seen in the thiazole nucleosides. These observations support the contention that, in solution, oxazofurin adopts a C-glycosidic bond conformation different from that seen in tiazofurin. The higher C-glycosidic angle in oxazofurin is primarily attributed to electrostatic repulsion between the furanose and oxazole oxygens.

Unlike tiazofurin, oxazofurin shows no in vitro cytotoxicity in either P388 or K562 cells.[9,18] Steric and hydrogen-bonding properties of the functional groups in the two compounds are similar. In particular, the carboxamide group, required for activity,[19] appears constrained to the same conformation in oxazofurin as that seen in the thiazole nucleosides.[14] Thus, it is likely that differences in activity are either (1) due directly to differences in electronic properties between the thiazole and oxazole rings or (2) due to the variation in C-glycosidic bond conformation resulting from the alteration in the charge distribution of the heterocycle.

Experimental Section

1. Crystallographic Study. Oxazofurin was prepared as described.[9] Colorless needle-shaped crystals were obtained by slow evaporation from a 7.5 mM oxazofurin solution in a 1-propanol/water mixture. Crystal data and data collection and refinement variables are listed in Table 1. One quadrant of data was collected at room temperature and corrected for Lorentz and polarization factors. Monitoring of three standard reflections showed no decay. Data were corrected for absorption using the semiempirical ψ-scan technique.[20] Equivalent reflections were averaged to give 6774 reflections, of which 5307 had $F_o > 3\sigma(F_o)$. However, *all* data were used in the subsequent refinements.

Initial attempts to phase the structure using standard direct methods multisolution techniques were unsuccessful, due to the severe overlap of atoms in the $hk0$ and $0kl$ projections. However, random phasing techniques[21] produced a number of early phase sets with strong, negative NQEST figures of merit.[22] Although additional refinement subsequently degraded, inspection of E maps from the earlier stages of refinement yielded recognizable fragments from four of the six conformers. Tangent formula recycling of this partial structure by random phasing methods[23] produced phase solutions that converged with stable NQEST values of ~−0.25. E maps from these solutions provided positions of all 102 non-hydrogen atoms, plus one water of hydration.

Positions of all 103 non-hydrogen atoms were refined with anisotropic temperature factors using full-matrix least-squares techniques. The oxazole proton and all methylene protons were added in idealized positions and refined using isotropic temperature factors. Positions of all carboxamide amino hydrogen atoms and positions of a number of hydroxyl protons were then obtained from successive difference Fourier maps, employing only low-angle data [$(\sin\theta)/\lambda < 0.4$ Å^{-1}].

Final refinements employed block-diagonal least squares. Six blocks were used, each block containing one molecule. The function minimized was $\sum w(\Delta F)^2$ where $\Delta F = |F_o| - |F_c|$. Weights were $w = 1/\sigma'^2$ where $\sigma' = [\sigma^2 + 0.5A|F_o|^2 + 0.5B[(\sin\theta)/\lambda]^2]^{1/2}$. Values of σ^2 were obtained from counting statistics. Values of A and B were obtained from least-squares minimization of the function $|\Delta F|^2 - \sigma'^2$ in 20 separate segments in $|F_o|$ and $(\sin\theta)/\lambda$ for the data set. Non-hydrogen atoms were refined anisotropically and positional parameters of all hydrogen atoms were refined with isotropic temperature factors. Final refinements included a type I extinction correction[24] and utilized all data. Atomic scattering factors were taken from ref 25. All refinement programs were from the DNA system.[26]

2. Computational Studies. Energy as a function of C-glycosidic torsion angle χ_o was computed for the oxazofurin model fragment using methods employed previously.[10,14] By analogy to tiazofurin, χ_o is defined by atoms O1′–C1′–C2–O1. A value of $\chi_o = 0°$ refers to the conformation in which the oxazole and furanose oxygen atoms are *cis*-planar. A positive value of χ_o indicates a counterclockwise rotation of the C2–O1 bond relative to the C1′–O1′ bond when viewed down the C-glycosidic bond from C2 to C1′.

Ab initio calculations were performed using the Gaussian90 system of programs and internal basis sets.[27] The value of χ_o was incremented in 10–20° steps and fixed. All remaining geometry variables describing the fragment were then optimized. Energy profiles were obtained using both symmetric and "ribose-like" fragments (see text). In the asymmetric "ribose-like" fragment, both the value of the CH3–O1′–C1′–C2 torsion angle as well as that of χ_o were fixed at each optimization. The initial fragment geometry in both models was based on the oxazofurin crystal structure. The starting geometry at each subsequent value of χ_o was the optimized geometry obtained at the previous value. All geometry optimizations used the analytical gradient method.[27]

Energies for the symmetric fragment were obtained for conformations between $\chi_o = 0°$ and 180° and the resulting energy

profile symmetrized about $\chi_o = 0°$. Energies for the asymmetric fragment were obtained for conformers between $\chi_0 = -180°$ and 180°. Optimized geometries and associated SCF energies were obtained using the 3-21G basis set for both the symmetric and "ribose-like" fragments. Thus, each point in Figure 3 represents a calculation at the RHF/3-21G//3-21G levels.[17]

In order to interpret the computed energy profiles and obtain estimated point charges, natural bond orbital (NBO) analyses were performed on model fragments using the NBO program incorporated in Gaussian90.[28] NBO analysis decomposes the internal energy of a chemical complex into a charge transfer energy resulting from electron delocalization and a non-charge-transfer energy, the latter including electrostatic and exclusion-repulsion terms.[28] NBO analyses were obtained for model fragments at $\chi_o = 0°$ (local maximum), 60° (global minimum), 140° (global maximum), and 180° (Figure 3).

Point charges were obtained from both thiazole and oxazole fragments using the natural population analysis method incorporated in the NBO program.[29] This method of charge partitioning uses fewer assumptions than the traditional Mulliken population analysis.[17,28,29] Charges were obtained from optimized geometries at the RHF level of theory using a 3-21G basis set for the oxazole fragment and a 3-21G* basis set for the sulfur-containing thiazole fragment.[17]

Acknowledgment. The authors thank Dr. Kenneth Haller for aid in the data collection. Work supported by Grants CA-45145 (B.M.G.) and GM-46733 (D.A.L.) from the National Institutes of Health, U.S. Department of Health and Human Services. Financial support from CNR, Italy, is also acknowledged.

Supplementary Material Available: Coordinates, thermal parameters, and bond lengths and angles for oxazofurin and listings of Browse Quantum Chemistry Database System[30] summaries for *ab initio* computations on model fragments (13 pages). Ordering information is given on any current masthead page.

References

(1) Jayaram, H. N.; Lapis, E.; Tricot, G. J.; Kneebone, P.; Paulik, E.; Zhen, W.; Engeler, G. P.; Hoffman, R.; Weber, G. Clinical Pharmacokinetic Study of Tiazofurin Administered as a 1-hour Infusion. *Int. J. Cancer* **1992**, *51*, 182–188.

(2) Tricot, G. J.; Jayaram, H. N.; Weber, G.; Hoffman, R. Tiazofurin: Biological Effects and Clinical Uses. *Int. J. Cell Cloning* **1990**, *8*, 161–170.

(3) Tricot, G. J.; Jayaram, H. N.; Lapis, E.; Natsumeda, Y.; Nichols, C. R.; Kneebone, P.; Heerema, N.; Weber, G.; Hoffman, R. Biochemically Directed Therapy of Leukemia with Tiazofurin, a Selective Blocker of Inosine 5′-Phosphate Dehydrogenase Activity. *Cancer Res.* **1989**, *49*, 3696–3701.

(4) (a) Weber, G.; Nagai, M.; Natsumeda, Y.; Eble, J. N.; Jayaram, H. N.; Paulik, E.; Zhen, W.; Hoffman, R.; Tricot, G. J. Tiazofurin Down-regulates Expression of c-Ki-ras Oncogene in a Leukemic Patient. *Cancer Commun.* **1991**, *3*, 61–66. (b) Goldstein, B. M.; Leary, J. F.; Farley, B. A.; Marquez, V. E.; Levy, P. C.; Rowley, P. T. Induction of HL60 Cell Differentiation by Tiazofurin and Its Analogues: Characterization and Efficacy. *Blood* **1991**, *78*, 593–598. (c) Kiguchi, K.; Collart, F. R.; Henning-Chubb, C.; Huberman, E. Cell Differentiation and Altered IMP Dehydrogenase Expression Induced in Human T-Lymphoblastoid Leukemia Cells by Mycophenolic Acid and Tiazofurin. *Exp. Cell Res.* **1990**, *187*, 47–53. (d) Sidi, Y.; Beery, E.; Panet, C.; Wasserman, L.; Novogrodsky, A.; Nordenberg, J. Growth Inhibition and Induction of Phenotypic Alterations by Tiazofurin: Differential Effects on MCF-7 Breast Cancer and HBL-100 Breast Cell Lines. *Eur. J. Cancer Clin. Oncol.* **1989**, *25*, 883–869. (e) Knight, R. D.; Mangum, J.; Lucas, D. L.; Cooney, D. A.; Khan, E. C.; Wright, D. G. Inosine Monophosphate Dehydrogenase and Myeloid Cell Maturation. *Blood* **1987**, *69*, 634–639. (f) Lucas, D. L.; Robins, R. K.; Knight, R. D.; Wright, D. G. Induced Maturation of the Human Promyelocytic Leukemia Cell Line, HL-60, by 2-β-D-Ribofuranosylselenazole-4-carboxamide. *Biochem. Biophys. Res. Commun.* **1983**, *115*, 971–980.

(5) Cooney, D. A.; Jayaram, H. N.; Gebeyehu, G.; Betts, C. R.; Kelley, J. A.; Marquez, V. E.; Johns, D. G. The Conversion of 2-β-D-Ribofuranosylthiazole-4-carboxamide to an Analogue of NAD with Potent IMP Dehydrogenase-Inhibitory Properties. *Biochem. Pharmacol.* **1982**, *31*, 2133–2136.

(6) Kuttan, R.; Robins, R. K.; Saunders, P. P. Inhibition of Inosinate Dehydrogenase by Metabolites of 2-β-D-Ribofuranosylthiazole-4-carboxamide. *Biochem. Biophys. Res. Commun.* **1982**, *107*, 862–868.

(7) Goldstein, B. M.; Takusagawa, F.; Berman, H. M.; Srivastava, P. C.; Robins, R. K. Structural Studies of a New Antitumor Agent: Tiazofurin and its Inactive Analogues. *J. Am. Chem. Soc.* **1983**, *105*, 7416–7422.

(8) Li, H.; Hallows, W. A.; Punzi, J. S.; Marquez, V. E.; Carrell, H. L.; Pankiewicz, K. W.; Watanabe, K. A.; Goldstein, B. M. Crystallographic Studies of Two Alcohol Dehydrogenase-Bound Analogues of Thiazole-4-Carboxamide Adenine Dinucleotide (TAD), the Active Anabolite of the Antitumor Agent Tiazofurin. *Biochemistry* **1994**, *33*, 23–32.

(9) Franchetti, P.; Cristalli, G.; Grifantini, M.; Cappellacci, L.; Vittori, S.; Nocentini, G. Synthesis and Antitumor Activity of 2-β-D-ribofuranosyloxazole-4-carboxamide (Oxazofurin). *J. Med. Chem.* **1990**, *33*, 2849–2852.

(10) Burling, F. T.; Goldstein, B. M. Computational Studies of Nonbonded Sulfur-Oxygen and Selenium-Oxygen Interactions in the Thiazole and Selenazole Nucleosides. *J. Am. Chem. Soc.* **1992**, *114*, 2313–2320.

(11) Burling, F. T.; Goldstein, B. M. A Database Study of Close Intramolecular Sulfur-Oxygen Contacts. *Acta Crystallogr., Sect. B* **1993**, *B49*, 738–744.

(12) Allen, F. H.; Kennard, O.; Taylor, R. Systematic Analysis of Structural Data as a Research Technique in Organic Chemistry. *Acc. Chem. Res.* **1983**, *16*, 146–153 and references therein.

(13) Saenger, W. *Principles of Nucleic Acid Structure*; Springer-Verlag: New York, 1984; Chapter 2.

(14) Li, H.; Goldstein, B. M. Carboxamide Group Conformation in the Nicotinamide and Thiazole-4-carboxamide Rings. Implications for Enzyme Binding. *J. Med. Chem.* **1992**, *35*, 3560–3567.

(15) (a) Burling, F. T.; Gabrielsen, B.; Goldstein, B. M. Structures of the 2′,3′-Dideoxy and 2′,3′-Didehydro-2′,3′-dideoxy Analogs of Tiazofurin. *Acta Crystallogr., Sect. C* **1991**, *C47*, 1272–1275. (b) Burling F. T.; Hallows W. H.; Phelan, M. J.; Gabrielsen, B.; Goldstein, B. M. Structures of the 4-Cyano and 4-Methylamidate Analogs of Tiazofurin. *Acta Crystallogr., Sect. B* **1992**, *B48*, 677–683.

(16) Goldstein, B. M.; Mao, D. T.; Marquez, V. E. Ara-tiazofurin: Conservation of Structural Features in an Unusual Thiazole Nucleoside. *J. Med. Chem.* **1988**, *31*, 1026–1031.

(17) Hehre, W. J.; Radom, L.; Schleyer, P. v. R.; Pople, J. A. *Ab. Initio Molecular Orbital Theory*; John Wiley-Interscience Publication: New York, 1986; Chapter 4.

(18) Jayaram, H. N. Unpublished results.

(19) Jayaram, H. N.; Dion, R. L.; Glazer, R. I.; Johns, D. G.; Robins, R. K.; Srivastava, P. C.; Cooney, D. A. Initial Studies on the Mechanism of Action of a New Oncolytic Thiazole Nucleoside, 2-β-D-Ribofuranosylthiazole-4-Carboxamide. *Biochem. Pharmacol.* **1982**, *31*, 2371–2380.

(20) North, A. C. T.; Phillips, D. C.; Mathews, F. S. A Semi-Empirical Method of Absorption Correction. *Acta Crystallogr., Sect. A* **1968**, *A24*, 351–359.

(21) Jia-Xing, Y. On the Application of Phase Relationships to Complex Structures. XVIII. RANTAN-Random MULTAN. *Acta Crystallogr., Sect. A* **1981**, *A37*, 642–644.

(22) DeTitta, G. T.; Edmonds, J. W.; Langs, D. A.; Hauptman, H. Use of Negative Quartet Cosine Invariants as a Phasing Figure of Merit: NQEST. *Acta Crystallogr., Sect. A* **1975**, *A31*, 472–479.

(23) Jia-Xing, Y. On the Application of Phase Relationships to Complex Structures. XX. RANTAN for Large Structures and Fragment Development. *Acta Crystallogr., Sect. A* **1983**, *A39*, 35–37.

(24) Coppens, P.; Hamilton, W. C. Anisotropic Extinction Corrections in the Zachariasen Approximation. *Acta Crystallogr., Sect. A* **1970**, *A26*, 71–83.

(25) *International Tables for X-ray Crystallography*, 3rd ed.; Kynoch Press: Birmingham, 1974 (present distributor Kluwer Academic Publishers, D. Reidel, Dordrecht); Vol. IV, pp 99 and 149.

(26) Takusagawa, F. *Crystallographic Computing System*: DNA; the Institute for Cancer Research: Fox Chase, PA, 1981.

(27) Frisch, M. J.; Head-Gordon, M.; Trucks, G. W.; Foresman, J. B.; Schlegel, H. B.; Raghavachari, K.; Robb, M. A.; Binkley, J. S.; Gonzalez, C.; Defrees, D. J.; Fox, D. J.; Whiteside, R. A.; Seeger, R.; Melius, C. F.; Baker, J.; Martin, R. L.; Kahn, L. R.; Stewart, J. J. P.; Topiol, S.; Pople, J. A. *Gaussian 90*; Gaussian, Inc., Pittsburgh, PA, 1990.

(28) (a) Reed, A. E.; Curtiss, L. A.; Weinhold, F. Intermolecular Interactions from a Natural Bond Orbital, Donor-Acceptor Viewpoint. *Chem. Rev.* **1988**, *88*, 889–926. (b) Glendening, E. D.; Reed, A. E.; Carpenter, J. E.; Weinhold, F., *NBO 3.0 Program Manual*; Theoretical Chemistry Institute and Department of Chemistry, University of Wisconsin: Madison, WI, 1990.

(29) Reed, A. E.; Weinstock, R.; Weinhold, F. Natural Population Analysis. *J. Chem. Phys.* **1985**, *83*, 735–746.

(30) Frisch, M. J. *Browse Quantum Chemistry Database System User's Guide*; Gaussian, Inc.: Pittsburgh, PA, 1988.